Nat Commun. Author manuscript; available in PMC 2016 April 26.

Published in final edited form as:
Nat Commun. ; 5: 4556. doi:10.1038/ncomms5556.

$G\alpha_s$ regulates the post-endocytic sorting of G protein-coupled receptors

Stéphanie Rosciglione, **Caroline Thériault**, **Marc-Olivier Boily**, **Marilène Paquette**, and **Christine Lavoie**[1]

Department of Pharmacology, Faculty of Medicine and Health Sciences, Université de Sherbrooke, Sherbrooke, QC, Canada

Abstract

The role of $G\alpha_s$ in G protein-coupled receptor (GPCR) signalling at the cell surface is well established. Recent evidence has revealed the presence of $G\alpha_s$ on endosomes and its capacity to elicit GPCR-promoted signalling from this intracellular compartment. Here, we report an unconventional role for $G\alpha_s$ in the endocytic sorting of GPCRs to lysosomes. Cellular depletion of $G\alpha_s$ specifically delays the lysosomal degradation of GPCRs by disrupting the transfer of GPCRs into the intraluminal vesicles (ILVs) of multivesicular bodies (MVBs). We show that $G\alpha_s$ interacts with GASP-1 and dysbindin, two key proteins that serve as linkers between GPCRs and the ESCRT (endosomal sorting complex required for transport) machinery involved in receptor sorting into ILVs. Our findings reveal that $G\alpha_s$ plays a role in both GPCR signalling and trafficking pathways, providing another piece in the intertwining molecular network between these processes.

Keywords

$G\alpha_s$; GPCR; multivesicular bodies (MVB); dysbindin; GASP-1; ESCRT; endosomal sorting

Introduction

Heterotrimeric G proteins, which are composed of α, β and γ subunits, transduce extracellular signals from G protein-coupled receptors (GPCRs) to intracellular downstream effector proteins. In the conventional G protein signalling paradigm, the G protein localises to the cytoplasmic surface of the plasma membrane (PM), where after activation by an agonist-bound GPCR, the GTP-bound Gα and free Gβγ bind to and regulate a number of

[1]Correspondence should be addressed to: Christine Lavoie, Department of Pharmacology, Institut de Pharmacologie de Sherbrooke, Faculty of Medicine, Université de Sherbrooke, 3001–12e Avenue Nord, Sherbrooke, QC, Canada, J1H 5N4, Telephone: 819-820-6868 ext. 12732, Fax: 819-564-5400, Christine.L.Lavoie@USherbrooke.ca.

Author Contributions

S.R. and C.L.L. designed the experiments, analysed the data and wrote the manuscript. S.R performed most of the experiments, with contributions from C.T. and C.L.L for certain immunofluorescence and GST pull-down experiments, M.O.B. for the generation of the constitutively active and inactive $G\alpha_s$ cDNA mutants and M.P. for the quantification of the endosomal fluorescence and colocalisation experiments.

Competing financial interests

The authors declare no competing financial interests.

well-studied effectors, including adenylyl cyclase, phospholipase Cβ and ion channels[1]. However, over the past decade, research has established that G proteins also have non-canonical roles in the cell, such as in regulating novel effectors[2–4], undergoing GPCR-independent activation[5] and acting on organelles[2–6]. Indeed, in addition to localising to the PM, heterotrimeric G proteins are found on the membranes of intracellular compartments along both the endocytic and secretory pathways, where mounting evidence suggests they play several roles in membrane trafficking[5,7–10].

Longstanding evidence have suggested that $G\alpha_s$ is involved in endosomal functions[11–14]. Several recent studies have confirmed that $G\alpha_s$ is present on endosomes and has non-conventional roles in endosomal receptor signalling and trafficking[15–19]. The ability of $G\alpha_s$ to be activated and signal from this intracellular compartment was recently observed following the internalisation of vasopressin type 2 receptor (V2R), parathyroid hormone receptor (PTHR) and β2-adrenergic receptor (β2AR), all of which are $G\alpha_s$-coupled GPCRs[15,16,20]. $G\alpha_s$ also regulates the endosomal sorting and down-regulation of epidermal growth factor receptor (EGFR), a single transmembrane-spanning receptor[18]. However, the role of $G\alpha_s$ in the endosomal sorting of other receptors, its precise molecular mechanism and the role of its activation status (GDP/GTP forms) in this trafficking step remain undefined.

GPCR activity is tightly controlled by endocytic pathway. Ligand-induced internalisation drives GPCRs into early endosomes, where they are either recycled back to the PM for another round of activation or sorted to the lysosomes for degradation, producing a prolonged attenuation of cellular signalling. Lysosomal sorting of GPCRs occurs via a highly conserved mechanism requiring recognition by the endosomal sorting complex required for transport (ESCRT), which sorts receptors into the intraluminal vesicles (ILVs) of multivesicular bodies (MVBs), leading to a point of no return for complete degradation in lysosomes[21,22]. Certain GPCRs are ubiquitinated, which regulates their direct interaction with the HRS component of the ESCRT machinery[23–25]. However, several GPCRs are sorted by the ESCRT machinery independent of ubiquitination[22,26,27]. Recent work has demonstrated that GPCR-associated binding protein-1 (GASP-1) and dysbindin link a subset of GPCRs to the ESCRT machinery. GASP-1 binds to the carboxyl-termini of several GPCRs and targets them to the lysosomal pathway[28–30]. Dysbindin, a cytoplasmic protein that functions in the biogenesis of specialised lysosome-related organelles, has recently been shown to promote the lysosomal sorting of δ-opioid receptor (DOP) and dopamine 2 receptor (D2R) and is thought to link GASP-1 to the HRS component of the ESCRT machinery[31]. A mechanistic understanding of GPCR endosomal sorting is only beginning to emerge.

In the present study, we investigated whether $G\alpha_s$ is involved in the regulation of the endocytic sorting of GPCRs. Our results showed that $G\alpha_s$ is critical for sorting GPCRs into the ILVs of MVBs through interactions with GASP-1, dysbindin and the ESCRT machinery. These interactions were independent of $G\alpha_s$ GTPase activity. This study defines a novel regulatory role for $G\alpha_s$ in the post-endocytic sorting and down-regulation of GPCRs.

Results

$G\alpha_s$ is required for the degradation of a subset of GPCRs

$G\alpha_s$ can localise to endosomes and participate in EGFR trafficking and signalling[17–19]. Because GPCRs are specifically sorted in endosomes, we investigated whether $G\alpha_s$ is involved in the endocytic trafficking of these receptors. We first analysed the impact of $G\alpha_s$ depletion on the basal levels of various GPCRs that are either sorted in the lysosomes (chemokine receptor type 4 (CXCR4), DOP, D2R and angiotensin 1 receptor (AT1R)) or recycled to the plasma membrane (β2AR, μ-opioid receptor (MOP) and dopamine 1 receptor (D1R)) (Fig. 1a). Tagged GPCRs were expressed in HEK293 cells transfected with control or $G\alpha_s$ siRNA, and Western blot analysis revealed that the expression levels of CXCR4, DOP, D2R and AT1R were increased in $G\alpha_s$-depleted cells, whereas the β2AR, MOP and D1R levels were unaffected. The quantification analysis confirmed the higher levels of lysosome-targeted GPCRs in steady state cells transfected with $G\alpha_s$ siRNA (Fig. 1b), suggesting that the basal turnover of these receptors was delayed by $G\alpha_s$ knockdown. This result was confirmed with endogenous CXCR4. $G\alpha_s$ depletion led to a significant increase in the steady state expression of endogenous CXCR4 in HeLa cells, a cell line that expresses high levels of endogenous CXCR4 and $G\alpha_s$ (Supplementary Fig. 1a), suggesting that $G\alpha_s$ similarly regulated the basal turnover of an endogenous GPCR. The specificity of the effect of $G\alpha_s$ on GPCR levels was validated in two different manners. First, the depletion of $G\alpha_{i3}$ and $G\beta_1$ did not affect the basal levels of HA-CXCR4 or HA-DOP (Supplementary Fig. 1b). Second, after reintroducing $G\alpha_s$ into $G\alpha_s$-depleted cells with siRNA-resistant forms of the short and long variants of human $G\alpha_s$, the basal levels of HA-CXCR4 and HA-DOP were similar to or lower than those in the control cells (Supplementary Fig. 1c), confirming a specific role for $G\alpha_s$ in influencing the levels of these particular GPCRs. Interestingly, all of the GPCRs that were affected by $G\alpha_s$ depletion are not coupled to $G\alpha_s$ in their conventional signalling pathways. Indeed, DOP, CXCR4 and D2R are coupled to $G\alpha_{i/o}$ [32–34], and AT1R is coupled to $G\alpha_{i/q}$ [35].

To determine whether the up-regulated GPCRs in steady state $G\alpha_s$-depleted cells localised to the PM, we measured the surface levels of these receptors as a function of $G\alpha_s$ expression. We focused on CXCR4 and DOP because these two GPCRs were most affected by $G\alpha_s$ depletion (Fig. 1a, b). A cell surface ELISA demonstrated that the cell surface expression of HA-DOP and HA-CXCR4 was significantly increased in $G\alpha_s$-depleted HEK293 cells (Fig. 1c). As the amount of a cell surface receptor is partly a function of the rate of receptor internalisation and recycling, we next examined the effect of $G\alpha_s$ depletion on the internalisation and recycling of HA-tagged CXCR4 and DOP by ELISA (Fig. 1d). No significant differences were observed between control and $G\alpha_s$-depleted cells (Fig. 1d), indicating that $G\alpha_s$ depletion had no effect on the internalisation and recycling of these GPCRs and suggesting that $G\alpha_s$ instead affected their constitutive trafficking and degradation. Accordingly, immunofluorescence microscopy analysis of the steady state distribution of HA-tagged CXCR4 in HEK293 cells showed an accumulation of CXCR4 in intracellular vesicles in $G\alpha_s$-depleted cells, whereas CXCR4 predominantly localised to the PM in control cells (Supplementary Fig. 1d). Together, these results suggested that the

increased steady state levels of CXCR4 and DOP in $G\alpha_s$-depleted cells were due to the involvement of $G\alpha_s$ in the constitutive trafficking and turnover of these receptors.

We next investigated whether $G\alpha_s$ depletion affected ligand-mediated GPCR trafficking and turnover. We assessed the effect of $G\alpha_s$ depletion on the kinetics of the ligand-dependent degradation of CXCR4 and DOP. Cells transiently overexpressing HA-tagged CXCR4 or DOP and transfected with control or $G\alpha_s$ siRNA were treated with agonists in the presence of cycloheximide (to block *de novo* protein synthesis) for the indicated time, and GPCR abundance was monitored by Western blot and quantified (Fig. 1e). In cells transfected with control siRNA, greater than 70% of the DOP and CXCR4 receptors were degraded after stimulation for 4 h or 2 h, respectively, whereas in cells transfected with $G\alpha_s$ siRNA, less than 20% of the receptors were degraded (Fig. 1e). The significantly reduced rate of receptor degradation in agonist-stimulated, $G\alpha_s$-depleted cells indicated a requirement for $G\alpha_s$ in the establishment of ligand-mediated GPCR turnover, suggesting that proper GPCR trafficking and sorting is dependent on $G\alpha_s$. Immunofluorescence microscopy was utilised to evaluate the effects of $G\alpha_s$ depletion on the endocytosis and degradation of cell surface labelled DOP and CXCR4 (Fig. 1f). After agonist stimulation for 60 min, the amount of DOP and CXCR4 that was internalised into vesicles was similar in control and $G\alpha_s$-depleted cells, confirming that $G\alpha_s$ depletion did not impair GPCR internalisation. However, after longer agonist treatments (120 or 180 min), cell surface labelled DOP and CXCR4 were mostly degraded in control cells but remained in intracellular vesicles in $G\alpha_s$-depleted cells (Fig. 1f). Together, these results suggested that the decreased degradation of DOP and CXCR4 in $G\alpha_s$-depleted cells was due to retention in intracellular compartments.

$G\alpha_s$ promotes GPCR sorting in the ILVs of MVBs

To identify the intracellular compartment in which DOP and CXCR4 were retained in $G\alpha_s$-depleted cells, we examined the distribution of internalised HA-tagged DOP and CXCR4 in control and $G\alpha_s$ siRNA-treated cells (Fig. 2a). After 15 min of agonist stimulation, cell surface labelled DOP and CXCR4 colocalised with the early endosomal marker EEA1 in both control and $G\alpha_s$-depleted cells. After 120 or 180 min of agonist stimulation, DOP and CXCR4 showed little colocalisation with EEA1 in control cells, consistent with receptor trafficking out of the early endosome to the late endosome/lysosomes. In contrast, DOP and CXCR4 exhibited robust colocalisation with EEA1 in $G\alpha_s$ siRNA-treated cells at this later timepoint. The quantitative analysis confirmed a significant increase in the colocalisation of DOP and CXCR4 with EEA1-positive endosomes in $G\alpha_s$-depleted cells compared with control cells (Fig. 2b). These results suggested that DOP and CXCR4 were trapped in early endosomes in the absence of $G\alpha_s$.

Following internalisation in early endosomes, GPCRs destined for lysosomal degradation, such as DOP and CXCR4, are transferred from the endosome limiting membranes to the ILVs of MVBs. We thus examined whether $G\alpha_s$ altered the sorting of GPCRs into ILVs. DOP and CXCR4 were tagged at their C-terminus with GFP (DOP-GFP) or CFP (CXCR4-CFP) and were co-expressed with constitutively active Rab5 (Rab5-Q79L) to create enlarged endosomes and to facilitate the detection of these GPCRs on the limiting and intraluminal membranes of MVBs (Fig. 2c). Confocal microscopy analysis of control cells stimulated

with agonist for 90 min showed the presence of DOP-GFP and CXCR4-CFP in both the limiting membranes and the ILVs of enlarged endosomes labelled with EEA1. In contrast, in $G\alpha_s$-depleted cells, DOP-GFP and CXCR4-CFP localised predominantly to the limiting membranes of enlarged endosomes, with most endosomes exhibiting little intraluminal fluorescence (Fig. 2d). The GPCR distribution across the endosomes was quantified by line scan analysis of confocal cross-sections as previously described[36]. A representative line scan analysis of an endosome is shown in Fig. 2e. The peaks indicate the limiting membrane, and the hatched box indicates the central region of the endosome lumen. An analysis of more than 100 endosomes from multiple cells and experiments revealed a 50% reduction in both DOP-GFP and CXCR4-CFP in the endosomal lumen in $G\alpha_s$-depleted cells compared with control cells (Fig. 2f). Taken together, these results indicated that $G\alpha_s$ plays a crucial role in the sorting of GPCRs in the ILVs of MVBs for subsequent lysosomal degradation.

$G\alpha_s$ is a component of the GPCR endosomal sorting machinery

To decipher the molecular mechanism by which $G\alpha_s$ regulates GPCR degradation, we next examined whether $G\alpha_s$ associates with the core machinery that mediates sorting into the ILVs of MVBs. ESCRT molecules, including HRS (ESCRT-0), are central players in the endosomal sorting of GPCRs[25,27]. HRS can either function directly by interacting with a ubiquitinated GPCR (such as CXCR4)[25] or indirectly by interacting with the accessory proteins GASP-1 and dysbindin, which are part of an alternate connectivity network linking particular GPCRs (such as DOP and D2R) to the ESCRT machinery[28–31]. To determine whether $G\alpha_s$ associates with these endocytic sorting components, HEK293 cells were transiently transfected with GFP or $G\alpha_s$-GFP together with untagged HRS, Myc-tagged dysbindin or Cherry-tagged GASP-1, and immunoprecipitations were performed with an anti-GFP antibody. $G\alpha_s$-GFP interacted with HRS, dysbindin and GASP-1 (Fig. 3a), suggesting that $G\alpha_s$ is part of this sorting machinery. These interactions were specific for $G\alpha_s$, as the $G\alpha$ proteins $G\alpha_{i3}$, $G\alpha_q$ and $G\alpha_z$ did not precipitate HRS, dysbindin or GASP-1 (Supplementary Fig. 2a).

We next examined whether the interactions between $G\alpha_s$ and the sorting machinery components are direct. ^{35}S-labelled, *in vitro*-translated GASP-1, dysbindin or HRS was incubated with glutathione beads coated with GST alone or with the short and long forms of $G\alpha_s$ fused to GST (GST-$G\alpha_s$ S/L). As shown in Fig. 3b, GST-$G\alpha_s$ bound to dysbindin and GASP-1 but not HRS, suggesting that $G\alpha_s$ bound directly to GASP-1 and dysbindin but required intermediate proteins to interact with HRS. Interestingly, dysbindin was identified by yeast two-hybrid as an interacting partner of HRS[37], suggesting that dysbindin could be the link between $G\alpha_s$ and HRS. However, direct interactions between dysbindin and HRS or between dysbindin and GASP-1 have not been confirmed. To better define the complex containing GASP-1, dysbindin, HRS and $G\alpha_s$, we generated GST-HRS and GST-GASP-1 and examined their interaction with ^{35}S-labelled, *in vitro*-translated $G\alpha_s$, GASP-1, dysbindin or HRS (Fig. 3c). We confirmed that dysbindin interacted directly with HRS and that $G\alpha_s$ interacted directly with GASP-1 but not with HRS. GASP-1 also interacted directly with HRS but not with dysbindin. These results indicated that although dysbindin and GASP-1 do not interact, they provide links between $G\alpha_s$ and HRS.

We next investigated the intracellular localisation of this protein complex. $G\alpha_s$ has been shown to localise with HRS on early endosomes[18]. To determine whether dysbindin and GASP-1 were present with $G\alpha_s$ on HRS-labelled endosomes, we performed immunofluorescent confocal microscopy on COS7 cells co-expressing $G\alpha_s$-GFP and Myc-dysbindin or Cherry-GASP-1 (Fig. 3d). Myc-dysbindin had a largely diffuse cytoplasmic distribution, but a fraction colocalised with $G\alpha_s$-GFP on HRS-positive endosomes. Similarly, Cherry-GASP-1 was mainly distributed throughout the cytoplasm but also colocalised with $G\alpha_s$-GFP and endogenous HRS on sorting endosomes. Interestingly, the overexpression of $G\alpha_s$ together with either dysbindin or GASP-1 altered the morphology of the early endosomes, as previously reported for overexpressed HRS [38–40]. Taken together, these data suggested that the components of this sorting complex localise together on early endosomes and could facilitate the sorting of GPCRs into the degradative pathway. In agreement with this hypothesis, we confirmed that internalised HA-DOP and HA-CXCR4 colocalised with $G\alpha_s$ on early endosomes (Supplementary Fig. 3).

$G\alpha_s$ activation state does not alter GPCR endosomal sorting

To determine whether the effect of $G\alpha_s$ on GPCR degradation depended on the GTPase activity of $G\alpha_s$, we investigated whether the interaction of $G\alpha_s$ with the sorting components dysbindin, GASP-1 and HRS depended on the activation state of $G\alpha_s$. Purified GST-$G\alpha_s$ or GST alone preloaded with GDP (to mimic the inactive state) or GDP/$AlF4^-$ or GTPγS (to mimic the active state) was incubated with ^{35}S-labelled, *in vitro*-translated GASP-1, dysbindin or HRS, and protein binding was analysed (Fig. 4a). Inactive and active GST-$G\alpha_s$ bound dysbindin and GASP-1 at similar levels and did not bind HRS, suggesting that the $G\alpha_s$ activation state did not influence these interactions. These results were confirmed using HEK293 cell lysates overexpressing Myc-dysbindin, Cherry-GASP-1 or untagged HRS (Fig. 4b). Again, the GST-$G\alpha_s$ interactions with dysbindin, GASP-1 and HRS were independent of the activation state of $G\alpha_s$. The small differences that were observed were not reproducible. The same results were obtained with immunoprecipitation assays using $G\alpha_s$-GFP mutants mimicking active or inactive $G\alpha_s$[41–43] (Supplementary Fig. 2b), indicating that the $G\alpha_s$ activation state did not influence its interactions with GASP-1, dysbindin and HRS.

The signalling-independent role of $G\alpha_s$ in GPCR endosomal sorting was next validated by determining whether the downstream effectors of $G\alpha_s$ altered CXCR4 down-regulation. Because $G\alpha_s$ stimulates cAMP production and protein kinase A (PKA) activation, we tested whether forskolin, an adenylate cyclase activator, could rescue $G\alpha_s$ depletion and whether H-89, a PKA inhibitor, could mimic $G\alpha_s$ depletion. Control and $G\alpha_s$-depleted HEK293 cells expressing HA-CXCR4 were treated with vehicle (DMSO), 10 μM forskolin or 10 μM H89 for 8–12 h. CXCR4 abundance was monitored by Western blot (Fig. 4c) and quantified using scanning densitometry to compare multiple independent experiments (Fig. 4d). PKA substrates were detected as a positive control for PKA activation (Fig. 4c). Although a significant increase in CXCR4 levels was observed in $G\alpha_s$-depleted cells treated with DMSO, no significant differences were observed between control cells (control siRNA) treated with H89 and vehicle (DMSO) (Fig 4d), indicating that PKA inactivation did not mimic $G\alpha_s$ depletion. Furthermore, no significant differences were observed between $G\alpha_s$

siRNA-treated cells incubated with forskolin or vehicle (Fig 4d), indicating that PKA activation did not rescue the effect of $G\alpha_s$ knockdown on CXCR4 levels, which would be expected if the inhibition of cAMP production in response to $G\alpha_s$ depletion was the cause of the increased CXCR4 levels. We concluded that $G\alpha_s$ activity and its downstream effectors did not play a major role in GPCR endocytic sorting and down-regulation.

Discussion

It is increasingly evident that endocytosis has numerous effects on GPCR signal transduction and that GPCR signalling regulates the endocytic machinery. This has blurred the traditional lines separating signalling and endocytosis at both the mechanistic and functional levels. Several proteins have been identified that function in both signalling and endocytosis, the best example being the β-arrestins, which mediate GPCR endocytosis by binding to AP2/clathrin and also participate in signal transduction by scaffolding components of the MAPK pathway[44–46]. The present study determined that $G\alpha_s$, which is usually involved in GPCR signalling, is a cellular regulator of the post-endocytic sorting of lysosome-targeted GPCRs.

This study indicated that $G\alpha_s$ is involved in the regulation of both basal turnover and ligand-mediated degradation of GPCRs. In steady state cells, $G\alpha_s$ depletion up-regulated the expression level of GPCRs that are specifically targeted to lysosomes (CXCR4, DOP, D2R and AT1R). Previous studies have shown that CXCR4 exhibits a high rate of constitutive internalisation and turnover [47,48], whereas other GPCRs, such as DOP, have a slow rate of constitutive internalisation and turnover [49]. These different turnover rates could explain why $G\alpha_s$ knockdown had a stronger effect on the basal levels of CXCR4. Further analysis of CXCR4 and DOP, which were most affected by $G\alpha_s$ depletion, indicated that $G\alpha_s$ depletion significantly inhibited their lysosomal proteolysis following ligand-stimulated endocytosis without noticeably affecting their internalisation and recycling rates. Furthermore, the reduced turnover of CXCR4 and DOP was accompanied by their accumulation on the cell surface and in early endosomes, suggesting a role for $G\alpha_s$ in the trafficking of these GPCRs through the sorting endosomes. The cellular phenotype after $G\alpha_s$ knockdown in this context closely resembled that observed when components of the ESCRT sorting machinery (such as HRS, AMSH and dysbindin) were perturbed [25,31,50], implying that $G\alpha_s$ is involved in the endosome sorting pathway for GPCR trafficking to lysosomes. Indeed, optical imaging demonstrated that $G\alpha_s$ depletion reduced the endosomal sorting of DOP and CXCR4 into the ILVs of MVBs, leading to the accumulation of DOP and CXCR4 on the limiting membranes of early endosomes and preventing receptor down-regulation.

This work provides the first molecular insight into the mechanism by which $G\alpha_s$ regulates the lysosomal sorting of GPCRs. Our results indicated that $G\alpha_s$ is required in both ubiquitin-dependent and ubiquitin-independent HRS-mediated GPCR sorting and suggested that $G\alpha_s$ is a scaffold for endosomal sorting components (Fig. 5). In this study, we determined that $G\alpha_s$ interacts directly with GASP-1 and dysbindin, two accessory sorting proteins that link a subset of GPCRs (such as DOP and D2R) to the HRS component of the ESCRT machinery in an ubiquitin-independent manner. Because the interactions between GASP-1, dysbindin and HRS have been previously reported but not clearly defined[31,37], we further characterised these interactions by showing that dysbindin interacts directly with HRS but not with

GASP-1 and that GASP-1 directly binds to HRS. Moreover, whereas human $G\alpha_s$ was previously shown to directly interact with rat HRS[18], no interaction was detected between human $G\alpha_s$ and human HRS, suggesting that this interactions is species-specific and is indirect in human cells. We propose that $G\alpha_s$ is present on early endosomes, where direct interactions with GASP-1 and dysbindin promote the downstream interaction of a subset of GPCRs with the ESCRT machinery (Fig. 5a). These interactions enable ubiquitin-independent sorting of these GPCRs into the ILVs of MVBs, resulting in lysosomal degradation. This model is supported by the fact that $G\alpha_s$ knockdown had similar effects on DOP and D2R lysosomal sorting and degradation as the knockdown of GASP-1[30,51,52], dysbindin[31] or HRS[27] (Supplementary Fig. 1b). The endosomal sorting role of $G\alpha_s$ was not restricted to GPCRs that interacted with GASP-1 and/or dysbindin. Indeed, the proteolytic down-regulation of CXCR4, which is sorted by the ubiquitin- and HRS-mediated ESCRT machinery[25] independent of GASP-1[53] and dysbindin (Supplementary Fig. 1b), was also affected by $G\alpha_s$ depletion. However, the molecular components of the CXCR4 endosomal sorting machinery that are regulated by $G\alpha_s$ have yet to be determined (Fig. 5b). Current studies are aimed at identifying this cofactor. Interestingly, the down-regulation of EGFR, which is also sorted by the ubiquitin-ESCRT machinery, has previously been shown to be altered by $G\alpha_s$ depletion[18], suggesting that $G\alpha_s$ acts on a general component of the endosomal sorting machinery for single and seven transmembrane receptors. Future studies should determine whether $G\alpha_s$ influences the down-regulation of other GPCRs, such as PAR1, that are sorted to lysosomes independent of ubiquitination, GASP-1 and certain late components of the ESCRT machinery[26,54,55]. Future studies should also refine our understanding of the role and significance of $G\alpha_s$ in general endosomal sorting.

$G\alpha_s$ activity is clearly not limited to the cell surface. Evidence from multiple studies has indicated that $G\alpha_s$ localises to the endosomes, where it has a functional role in both receptor signalling and trafficking. The presence of $G\alpha_s$ on endosomes has been known for more than a decade, but its role on this intracellular compartment is only beginning to emerge. $G\alpha_s$ is now known to mediate functionally significant signalling from endosomes. Various GPCRs (e.g., TSHR, PTHR, D1R and β2AR) signal via the $G\alpha_s$-linked activation of adenylyl cyclase directly from the endosome membrane[15,20,56,57]. Moreover, the active forms of β2AR and $G\alpha_s$ have been clearly visualised on endosomes[15]. $G\alpha_s$ has also been implicated in endosomal membrane trafficking functions, such as endosome fusion, pIgR transcytosis and EGFR down-regulation[11–14,18,19]. An important question is whether the GTPase activity of $G\alpha_s$ is involved in endosomal trafficking. It was previously reported that inactive $G\alpha_s$ interacted with GIV/girdin and was involved in EEA1 membrane recruitment (for EGFR trafficking)[19] and that the active state of $G\alpha_s$ negatively regulated endosomal fusion[14]. However, in our study, the $G\alpha_s$ activation state did not affect the interactions with the endosomal sorting machinery (GASP-1, dysbindin and HRS). Consistent with these findings, the effect of $G\alpha_s$ was independent of the $G\alpha_s$ signalling effectors adenylyl cyclase and PKA, supporting an activation state-independent role for $G\alpha_s$. These results support a scaffolding, rather than a signalling role for $G\alpha_s$ in GPCR degradation. Interestingly, we noted that none of the GPCRs affected by $G\alpha_s$ depletion are coupled to $G\alpha_s$ for signalling. Indeed, GPCRs coupled to $G\alpha_s$ are sorted to the PM following endocytosis. In fact, we were unable to identify a GPCR coupled to $G\alpha_s$ that is normally sorted to lysosomes. It is

possible that the endosomal activation of $G\alpha_s$ by these receptors prevents their interaction with the lysosomal sorting machinery, or perhaps the $G\alpha_s$ sorting step occurs later in endosomal maturation, when the recycling GPCRs have already been removed. We intend to investigate these intriguing hypotheses in future studies. The mechanism by which $G\alpha_s$ is translocated to endosomes remains unknown. One possibility is that the activation of a $G\alpha_s$-linked GPCR stimulates translocation. Following β2AR activation or cholera toxin treatment, $G\alpha_s$ has been shown to dissociate from the PM through activation-induced depalmitoylation of $G\alpha_s$[58–62]. Another possibility is that $G\alpha_s$ is internalised through the endocytic pathway. Following agonist stimulation, $G\alpha_s$ has been shown to localise to vesicles derived from the PM that do not contain β2AR, suggesting that β2AR and $G\alpha_s$ traffic through distinct endocytic pathways[63,64]. However, partial colocalisation of $G\alpha_s$ with β2AR has been observed on early endosomes[15,63], which corresponds with our data indicating that $G\alpha_s$ colocalises with DOP or CXCR4 on endosomes. Further studies are necessary to determine whether the stimulation of GPCRs that do not activate $G\alpha_s$, such as DOP, leads to the translocation of $G\alpha_s$ to the endosomal membrane or whether the stimulation of a $G\alpha_s$-coupled GPCR increases the translocation of $G\alpha_s$ to endosomes, thereby modulating the lysosomal degradation of other GPCRs.

Our findings raise the attractive possibility that $G\alpha_s$ plays a role in both GPCR signalling and trafficking pathways, providing another piece to the intertwining molecular network between these processes. Thus, it is tempting to speculate that $G\alpha_s$ plays a dual role in GPCR signalling via a rapidly responding second messenger system and via the regulation of GPCR lysosomal trafficking and down-regulation.

Methods

Antibodies and Reagents

The following antibodies were used in this study: anti-HA monoclonal antibody (mAb) (1:1000 for western blot (WB) and 1:500 for immunofluorescence (IF); Covance, Emeryville, CA, USA), anti-Flag M1 and M2 mAbs and polyclonal antibodies (pAbs) (1:1000 for WB and 1:500 for IF; Sigma-Aldrich, Saint Louis, MO, USA), anti-$G\alpha_s$ pAb (1:1000 for WB; Calbiochem, San Diego, CA, USA), anti-HRS mAbs (1:100 for IF; Alexis Biochemicals, San Diego, CA, USA) and pAbs (1:1000 for WB and 1:100 for IF; Millipore, Billerica, MA, USA), anti-GFP mAbs (1:3000 for WB and 1:500 for IF; Clontech, Mountain View, CA, USA) and pAbs (1:3000 for WB and 1:500 for IF; Invitrogen, Carlsbad, CA, USA), anti-EEA1 pAbs (1:1000 for WB and 1:100 for IF; Thermo Scientific, Rockford, IL, USA), anti-EEA1 goat Abs (1:100 for IF), anti-$G\alpha_i3$ and anti-Gβ1 pAbs (1:1000 for WB) (Santa Cruz Biotechnology, Santa Cruz, CA, USA), anti-CXCR4 (CD184; 1:1000 for WB; BD, Franklin Lakes, NJ, USA) and anti-Myc pAbs (1:2000 for WB and 1:1000 for IF; Upstate, Temecula, CA, USA). The anti-dysbindin (1:500 for WB) and anti-GASP-1 (1:10 000 for WB and 1:2000 for IF) pAbs were generous gifts from Dr Koh-Ichi Nagata (Institute for Developmental Research, Aichi Human Service Center, Japan) and Dr Frédéric Simonin (Université de Strasbourg, France), respectively.

DNA Constructs

pCDNA3.1 vectors expressing either the long (L) or short (S) forms of $G\alpha_s$ were obtained from the Guthrie cDNA Resource Center (Missouri University of Science and Technology, Rolla, MO). The $G\alpha_s$-GFP fusion protein was a generous gift from Dr Mark Rasenick (University of Illinois, Chicago, IL, USA) and has been previously described [62]. The constitutively active $G\alpha_s$ mutant (Q227L) and constitutively inactive $G\alpha_s$ mutant (G226A, R280K, T284D, I285T and A366S) were generated from $G\alpha_s$-GFP cDNA by QuickChange site-directed mutagenesis as previously described[41–43]. siRNA-resistant forms of the WT, active and inactive $G\alpha_s$ constructs were created by introducing silent substitutions into the $G\alpha_s$ or $G\alpha_s$-GFP cDNAs within the region of homology to the siRNA $G\alpha_s$ oligo, as previously described [18]. pcDNA3-$G\alpha_{i3}$-YFP has been previously described [65], and pcDNA3-$G\alpha_q$ and pcDNA3-$G\alpha_z$ were purchased from the Guthrie cDNA Resource Center (Missouri University of Science and Technology, Rolla, MO, USA) and subcloned into pEGFP-N1. pRK5-Myc-dysbindin was obtained from Dr Koh-Ichi Nagata (Institute for Developmental Research, Aichi Human Service Center, Japan), and untagged dysbindin was generated by subcloning into pcDNA3 and pGEX-KG. pcDNA3-Cherry-GASP-1 and pGEX-GASP-1 were obtained from Dr Frédéric Simonin (Université de Strasbourg, France), and untagged GASP-1 was obtained by subcloning into pcDNA3. pCS2-HRS-RFP was purchased from Addgene (Cambridge, MA, USA), and untagged HRS was subcloned into pcDNA3 and pGEX-KG. pcDNA3-HA-CXCR4 and pcDNA3-HA-β2AR were obtained from Dr Jean-Luc Parent (Université de Sherbrooke, Qc, Canada). pcDNA3-Flag-AT1R and pEGFP-C1-DOP were obtained from Dr Richard Leduc and Dr Louis Gendron (Université de Sherbrooke, Qc, Canada), respectively. pECFP-C1-CXCR4 was a generous gift from Dr Richard Miller (Northwestern University, Chicago, IL, USA). pcDNA3.1-3*HA-DOP, pcDNA3.1-HA-D1R and pcDNA3.1-HA-D2R were purchased from Missouri S&T, cDNA Resource Center (Missouri University of Science and Technology, Rolla, MO, USA).

Cell Culture and Transfection

COS7 cells were obtained from Dr Klaus Hahn (University of North Carolina, NC, USA), and HEK293T cells were obtained from Dr Alexandra Newton (University of California, San Diego, CA, USA). HEK293 cells stably expressing Flag-DOP or Flag-MOP were obtained from Dr Richard Howells (New Jersey Medical School, Newark, NJ, USA). The cells were grown in DMEM high glucose (Invitrogen, Carlsbad, CA, USA) containing 10% FBS (Hyclone Laboratories, Logan, UT, USA), penicillin and streptomycin. G418 (200 μg/ml, Invitrogen) was added to the culture medium for the stable cell lines. Cells were transfected using Lipofectamine 2000 (Invitrogen), X-TremeGENE HP or Fugene 6 (Roche Diagnostic, Indianapolis, IN, USA) according to the manufacturers' instructions.

RNA Interference and Rescue

Scrambled RNA oligos (scramble II duplex) and siRNAs against $G\alpha_s$ (previously described in Zheng et al, 2004 [18]), $G\alpha_{i3}$, $G\beta_1$ and HRS were purchased from Dharmacon (Lafayette, CO), and dysbindin siRNA was purchased from Qiagen (Hilden, Germany). HEK293T cells were transfected with a final concentration of 100 nM siRNA duplex using Lipofectamine 2000 (Invitrogen) according to the manufacturer's instructions. The cells were analysed 72 h

after the siRNA transfection. The various tagged GPCR cDNAs were transfected using X-tremeGENE HP 48h before the cell lysis or IF experiments. Rescue experiments were performed by transfecting the cells with cDNAs encoding siRNA-resistant forms of untagged $G\alpha_s$ (short and long) or with control vectors (pcDNA3) using X-tremeGENE HP 10h after the initial human $G\alpha_s$ siRNA transfection.

GPCRs Basal Expression and Degradation Assay

For the basal expression analysis, HEK293T cells were treated with the $G\alpha_s$ siRNA duplex and transfected with the various tagged GPCRs (as described above). Seventy-two hours after the initial siRNA transfection, all the cells were lysed in RIPA Buffer (50 mM Tris-HCl, pH 8, 150 mM NaCl, 1% NP40, 0.1% sodium deoxycholate, 5 mM EDTA and complete protease inhibitors (Roche, Basel, Switzerland)), with the exception of the Flag-DOP and Flag-MOP stable cell lines, which were lysed in OR buffer (150 mM Tris-HCl, pH 7.5, 300 mM NaCl, 1mM $MgCl_2$, 1mM $CaCl_2$, 1% Triton X-100, 10% glycerol and complete protease inhibitors) as previously described [66]. The lysates were incubated for 1 h at 4°C and centrifuged at 15,000 xg for 20 min at 4°C. The supernatants were recovered, and the protein concentrations were evaluated by Bradford assay. Thirty micrograms of each protein sample was aliquoted in Laemmli sample buffer and analysed by immunoblotting. For the degradation assays, HEK cells were treated with the $G\alpha_s$ siRNA duplex and transfected with HA-CXCR4 or HA-DOP (as described above). Forty-eight hours after the initial siRNA treatment, the cells were passaged onto poly-L-Lysine-coated 6-well plates (Sigma-Aldrich, Saint Louis, MO, USA) and grown for an additional 24 h. The cells were washed and incubated with DMEM containing 25 mM Hepes, 0.2% BSA and 50 μg/mL cycloheximide for 15 min at 37°C. The cells were then incubated with the same medium supplemented with agonist (100 nM SDF1-α or 5 μM DPDPE) for various periods of time. The cells were washed with ice-cold PBS and lysed in RIPA buffer. The lysates were processed as described above and were analysed by immunoblotting.

Cell Surface ELISA

Cell surface ELISAs were performed as previously described [67]. HEK cells were treated with the $G\alpha_s$ siRNA duplex and transfected with HA-CXCR4 or HA-DOP (as described above, 2 μg/P10 dish). Forty-eight hours after the initial siRNA treatment, the cells were plated onto poly-L-Lysine-coated 24-well plates (Sigma-Aldrich, Saint Louis, MO, USA). After 24 h, the cells were starved for 1 h at 37°C in DMEM and then incubated with DMEM containing 25 mM Hepes, 0.2% BSA and agonist (100 nM SDF1-α or 5 μM DPDPE) for 30 min or agonist for 30 min followed by antagonist (10 μM Naloxone or AMD3100) for 60 min. The cells were then fixed with 3% formaldehyde, washed with TBS, blocked in 5% BSA and incubated for 1 h with primary antibody (monoclonal anti-HA antibody) and for 45 min with secondary antibody (alkaline phosphatase-conjugated goat anti-mouse antibody; Sigma-Aldrich, Saint-Louis, MO, USA). The cells were then washed three times, and 250 μl of a colorimetric alkaline phosphatase substrate (diethanolamine and phosphatase substrate; Sigma-Aldrich, Saint-Louis, MO, USA) was added. The plates were incubated at 37°C for the appropriate time, and then 250 μl of NaOH (0.4 M) was added to stop the reaction. A 100-μl aliquot of the colorimetric reaction was collected, and the absorbance was measured at 405 nm using a spectrophotometer (Titertek Multiskan MCC/340; Labsystems).

Immunoblotting

The protein samples were separated on 8 or 10% SDS-PAGE gels and transferred to nitrocellulose membranes (Perkin Elmer, Waltham, Massachusetts, USA). The membranes were blocked in Tris-buffered saline (20 mM Tris-HCl, pH 7.4, and 150 mM NaCl) containing 0.1% Tween 20 and 5% nonfat dry milk, incubated with primary antibodies for 1 h at room temperature or overnight at 4°C, subsequently incubated with horseradish peroxidase-conjugated goat anti-rabbit or anti-mouse IgG (Bio-Rad, Hercules, CA, USA) and enhanced using a chemiluminescence detection reagent (Pierce Chemical, Thermo Fisher Scientific, Waltham, Massachusetts, USA).

Immunofluorescence

HEK or COS7 cells were grown on coverslips. Twenty-four to seventy-two hours after transfection, the cells were fixed with 3% paraformaldehyde (PFA) in 100 mM phosphate buffer, pH 7.4, for 30 min, permeabilised with 0.1% Triton-X100 for 10 min, blocked with 10% FBS or goat serum for 30 min, incubated with primary antibodies for 1 h at RT and incubated with Alexa Fluor-conjugated secondary antibodies (Molecular Probes, OR). The cells were visualised using an inverted confocal laser scanning microscope (FV1000; Olympus, Tokyo, Japan) equipped with a PlanApo 60x/1.42 oil immersion objective. Olympus FluoView version 1.6a was used to acquire and analyse the images, which were further processed using Adobe Photoshop (Adobe Systems, San Jose, CA, USA). The degree of colocalisation between fluorescently labelled GPCRs and the early endosome marker EEA1 was quantified by calculating the Manders coefficient [68] using Olympus FluoView v1.6b colocalisation software. The quantitative analysis was performed on 30 size-matched cells for each experimental condition, and the experiments were performed twice.

Quantification of DOP-GFP Localisation in the Endosomal Lumen

HEK cells treated with the control or $G\alpha_s$ siRNA duplex were transfected with DOP-GFP or CXCR4-CFP along with Rab5-Q79L to create enlarged endosomes. Forty-eight hours later, the cells were plated onto poly-L-Lysine-coated coverslips and incubated in the presence of 5 μM DPDPE or 100 nM SDF1-α for 90 min prior to fixation, processing for IF and image acquisition. To quantify the presence of DOP-GFP and CXCR4-CFP in the ILVs of endosomes, measurements were taken from raw data on individual endosomes as previously described [36,69]. The quantification was performed on raw data representing confocal cross-sections of individual endosomes. For each endosome, straight-line selections were drawn across the diameter, and pixel intensities across the line were measured. The endosomal diameter was normalised to account for different endosome sizes. The pixel numbers with the first and second maximum pixel intensities, corresponding to pixels on the limiting membrane of the endosome, were normalised to 0 and 100, respectively. The location across the line of pixel 0 was then subtracted from each pixel situated on the line, and this value was divided by the total diameter (in pixels) of the endosome. This generated normalised pixel distances corresponding to the distance across the line occupied by each pixel and was expressed as a percentage. The average background fluorescence was subtracted from the raw pixel intensity values. The pixel intensities for the pixel numbers normalised to 0 and

100 were also normalised to 0 and 100, respectively, generating normalised fluorescence values. The background-corrected pixel intensity values corresponding to pixels that lay 40–60% across the endosomal diameter were averaged, generating a middle fluorescence value for each endosome. The middle fluorescence values for multiple cells were compiled, and the mean for each condition is shown. Representative live images were rendered using Adobe Photoshop software.

Antibody Uptake Assay

HEK cells were treated with the control or $G\alpha_s$ siRNA duplex and transfected with HA-CXCR4 or HA-DOP (as described above). Forty-eight hours after the initial siRNA treatment, the cells were passaged onto poly-L-Lysine-coated coverslips (BD Bioscience, Franklin Lakes, NJ, USA) and grown for an additional 24 h. After serum starvation for 1 h, the cells were incubated on ice for 1 h with DMEM containing 25 mM Hepes, 0.2% BSA and anti-HA or anti-Flag (for stable cells) antibody (1:500 dilution). The cells were washed in ice-cold DMEM containing 25 mM Hepes and 0.2% BSA and were incubated at 37°C with the same medium supplemented with agonist (100 nM SDF1-α or 5 μM DPDPE) for different times. Subsequently, the cells were fixed and processed for IF. To enable the direct comparison of the Flag-DOP or HA-CXCR4 levels remaining in the cells following agonist treatment for different periods of time, all the images within a given experiment were taken with the same magnification and laser intensity settings.

Co-Immunoprecipitation

HEK cells were transiently transfected with GFP or $G\alpha_s$-GFP together with HRS, Myc-dysbindin or Cherry-GASP-1 cDNA. Forty-eight hours later, the cells were washed twice with ice-cold PBS, lysed in 50 mM Tris-HCl pH 7.4, containing 150 mM NaCl, 1% NP40 and protease inhibitors for 1 h at 4°C and centrifuged at 15,000 xg for 20 min. The cleared supernatants were incubated with primary antibodies (1 μg of antibody per 1 mg of protein) overnight at 4°C and then with protein A-Sepharose (GE Healthcare, Piscataway, NJ, USA) or protein G-Sepharose (Zymed, San Francisco, CA, USA) beads for 1 h. The beads were washed three times in lysis buffer and then boiled in Laemmli sample buffer. Bound immune complexes were analysed by SDS-PAGE and immunoblotting.

Glutathione S-Transferase Pull-Down Assays

GST fusion proteins were expressed in *E. coli* BL21 cells and purified on glutathione-Sepharose 4B beads (Pharmacia, Piscataway, NJ, USA) as previously described[70]. The ^{35}S-labelled *in vitro* translation products of pcDNA3-dysbindin, pcDNA3-GASP-1 and pcDNA3-HRS were prepared using the TNT T7 rabbit reticulocyte Quick Coupled Transcription/Translation system (Promega, San Luis Obispo, CA, USA) in the presence of [^{35}S]EasyTag EXPRESS labelling mix (73% Met/22% Cys; >1000 Ci/mmol, Perkin Elmer). A total of 5–10 μg of purified GST or GST-fusion protein was incubated with the *in vitro* translated products in 20 mM Tris, pH 7.4, 150 mM NaCl, 3 mM EDTA, 0.1% NP40, 1 mM DTT and complete protease inhibitor for 2 h at 4°C and washed four times with the same buffer. Bound proteins were eluted with Laemmli buffer, resolved by SDS-PAGE and visualised by autoradiography. For the GST pull-down assays on cell lysates, purified GST-proteins were incubated with 1 mg of lysate from HEK cells expressing Myc-dysbindin,

Cherry-GASP-1, untagged HRS or $G\alpha_s$ (S/L) that was prepared as described in the co-immunoprecipitation section. The bound proteins were separated by SDS-PAGE and detected by immunoblotting. In the experiments involving nucleotide loading, GST-$G\alpha_s$ was preincubated with 30 μM GDP alone, 30 μM GDP, 30 μM $AlCl_3$ and 10 mM NaF (GDP +$AlF4^-$), or 30 μM GTPγS in binding buffer (50 mM Tris-HCl, pH 7.4, 100 mM NaCl, 5 mM EDTA, 0.4% NP-40, 2 mM DTT, 10 mM $MgCl_2$ and protease inhibitors) for 90 min at room temperature before incubation with *in vitro* translated proteins or cell lysates. The washing buffer was supplemented with GDP alone, GDP, $AlCl_3$ and NaF or GTPγs, as during the binding, as previously described [19,70]. Bound proteins were either immunoblotted or exposed for autoradiography.

Statistical Analysis

The western blot quantification was performed using Image-Pro Plus Quantification 6.0 software. The GPCR band pixels were normalised to the EEA1 band pixels. Experiments were performed in triplicate, and the results are presented as the mean±SD. The statistical significance of the differences between the samples was assessed using Student's *t* test. A value of $p<0.05$ was considered significant.

Supplementary Material

Refer to Web version on PubMed Central for supplementary material.

Acknowledgments

We are grateful to Koh-Ichi Nagata (Aichi Human Service Center), Frédéric Simonin (Université de Strasbourg), Richard Howells (New Jersey Medical School), Richard Miller (Northwestern University), Richard Leduc, Jean-Luc Parent and Louis Gendron (Université de Sherbrooke) for generous gifts of antibodies, cDNA and cell lines. We also thank Jade Degrandmaison for the rapid development of ELISAs and Jean-Luc Parent for constructive comments on the manuscript. This work was supported by grant MOP-97936 from the Canadian Institutes of Health Research and a Canada Research Chair in Cellular Pharmacology (to C.L.L.).

References

1. Musnier A, Blanchot B, Reiter E, Crepieux P. GPCR signalling to the translation machinery. Cell Signal. 2010; 22:707–16. [PubMed: 19887105]
2. Robitaille M, et al. Gbetagamma is a negative regulator of AP-1 mediated transcription. Cell Signal. 2010; 22:1254–66. [PubMed: 20403427]
3. Hewavitharana T, Wedegaertner PB. Non-canonical signaling and localizations of heterotrimeric G proteins. Cell Signal. 2012; 24:25–34. [PubMed: 21907280]
4. Dupre DJ, Robitaille M, Rebois RV, Hebert TE. The role of Gbetagamma subunits in the organization, assembly, and function of GPCR signaling complexes. Annu Rev Pharmacol Toxicol. 2009; 49:31–56. [PubMed: 18834311]
5. Giannotta M, et al. The KDEL receptor couples to Galphaq/11 to activate Src kinases and regulate transport through the Golgi. Embo J. 2012; 31:2869–81. [PubMed: 22580821]
6. Khan SM, et al. The expanding roles of Gbetagamma subunits in G protein-coupled receptor signaling and drug action. Pharmacol Rev. 2013; 65:545–77. [PubMed: 23406670]
7. Irannejad R, Wedegaertner PB. Regulation of constitutive cargo transport from the trans-Golgi network to plasma membrane by Golgi-localized G protein betagamma subunits. J Biol Chem. 2010; 285:32393–404. [PubMed: 20720014]
8. Stow JL, Heimann K. Vesicle budding on Golgi membranes: regulation by G proteins and myosin motors. Biochim Biophys Acta. 1998; 1404:161–71. [PubMed: 9714787]

9. Nurnberg B, Ahnert-Hilger G. Potential roles of heterotrimeric G proteins of the endomembrane system. FEBS Lett. 1996; 389:61–5. [PubMed: 8682207]
10. Bomsel M, Mostov K. Role of heterotrimeric G proteins in membrane traffic. Mol Biol Cell. 1992; 3:1317–28. [PubMed: 1493332]
11. Bomsel M, Mostov KE. Possible role of both the alpha and beta gamma subunits of the heterotrimeric G protein, Gs, in transcytosis of the polymeric immunoglobulin receptor. J Biol Chem. 1993; 268:25824–35. [PubMed: 8245019]
12. Beron W, Colombo MI, Mayorga LS, Stahl PD. In vitro reconstitution of phagosome-endosome fusion: evidence for regulation by heterotrimeric GTPases. Arch Biochem Biophys. 1995; 317:337–42. [PubMed: 7893147]
13. Colombo MI, Mayorga LS, Casey PJ, Stahl PD. Evidence of a role for heterotrimeric GTP-binding proteins in endosome fusion. Science. 1992; 255:1695–7. [PubMed: 1348148]
14. Colombo MI, Mayorga LS, Nishimoto I, Ross EM, Stahl PD. Gs regulation of endosome fusion suggests a role for signal transduction pathways in endocytosis. J Biol Chem. 1994; 269:14919–23. [PubMed: 8195123]
15. Irannejad R, et al. Conformational biosensors reveal GPCR signalling from endosomes. Nature. 2013; 495:534–8. [PubMed: 23515162]
16. Feinstein TN, et al. Noncanonical control of vasopressin receptor type 2 signaling by retromer and arrestin. J Biol Chem. 2013; 288:27849–60. [PubMed: 23935101]
17. Van Dyke RW. Heterotrimeric G protein subunits are located on rat liver endosomes. BMC Physiol. 2004; 4:1. [PubMed: 14711382]
18. Zheng B, et al. Regulation of epidermal growth factor receptor degradation by heterotrimeric Galphas protein. Mol Biol Cell. 2004; 15:5538–50. [PubMed: 15469987]
19. Beas AO, et al. Galphas promotes EEA1 endosome maturation and shuts down proliferative signaling through interaction with GIV (Girdin). Mol Biol Cell. 2012; 23:4623–34. [PubMed: 23051738]
20. Ferrandon S, et al. Sustained cyclic AMP production by parathyroid hormone receptor endocytosis. Nat Chem Biol. 2009; 5:734–42. [PubMed: 19701185]
21. Wollert T, Hurley JH. Molecular mechanism of multivesicular body biogenesis by ESCRT complexes. Nature. 2010; 464:864–9. [PubMed: 20305637]
22. Hanyaloglu AC, von Zastrow M. Regulation of GPCRs by endocytic membrane trafficking and its potential implications. Annu Rev Pharmacol Toxicol. 2008; 48:537–68. [PubMed: 18184106]
23. Giordano F, Simoes S, Raposo G. The ocular albinism type 1 (OA1) GPCR is ubiquitinated and its traffic requires endosomal sorting complex responsible for transport (ESCRT) function. Proc Natl Acad Sci U S A. 2011; 108:11906–11. [PubMed: 21730137]
24. Hasdemir B, Bunnett NW, Cottrell GS. Hepatocyte growth factor-regulated tyrosine kinase substrate (HRS) mediates post-endocytic trafficking of protease-activated receptor 2 and calcitonin receptor-like receptor. J Biol Chem. 2007; 282:29646–57. [PubMed: 17675298]
25. Marchese A, et al. The E3 ubiquitin ligase AIP4 mediates ubiquitination and sorting of the G protein-coupled receptor CXCR4. Dev Cell. 2003; 5:709–22. [PubMed: 14602072]
26. Dores MR, et al. ALIX binds a YPX(3)L motif of the GPCR PAR1 and mediates ubiquitin-independent ESCRT-III/MVB sorting. J Cell Biol. 2012; 197:407–19. [PubMed: 22547407]
27. Hislop JN, Marley A, Von Zastrow M. Role of mammalian vacuolar protein-sorting proteins in endocytic trafficking of a non-ubiquitinated G protein-coupled receptor to lysosomes. J Biol Chem. 2004; 279:22522–31. [PubMed: 15024011]
28. Whistler JL, et al. Modulation of postendocytic sorting of G protein-coupled receptors. Science. 2002; 297:615–20. [PubMed: 12142540]
29. Simonin F, Karcher P, Boeuf JJ, Matifas A, Kieffer BL. Identification of a novel family of G protein-coupled receptor associated sorting proteins. J Neurochem. 2004; 89:766–75. [PubMed: 15086532]
30. Bornert O, et al. Identification of a novel protein-protein interaction motif mediating interaction of GPCR-associated sorting proteins with G protein-coupled receptors. PLoS One. 2013; 8:e56336. [PubMed: 23441177]

31. Marley A, von Zastrow M. Dysbindin promotes the post-endocytic sorting of G protein-coupled receptors to lysosomes. PLoS One. 2010; 5:e9325. [PubMed: 20174469]
32. Prather PL, Loh HH, Law PY. Interaction of delta-opioid receptors with multiple G proteins: a non-relationship between agonist potency to inhibit adenylyl cyclase and to activate G proteins. Mol Pharmacol. 1994; 45:997–1003. [PubMed: 8190115]
33. Moepps B, Frodl R, Rodewald HR, Baggiolini M, Gierschik P. Two murine homologues of the human chemokine receptor CXCR4 mediating stromal cell-derived factor 1alpha activation of Gi2 are differentially expressed in vivo. Eur J Immunol. 1997; 27:2102–12. [PubMed: 9295051]
34. Montmayeur JP, Borrelli E. Transcription mediated by a cAMP-responsive promoter element is reduced upon activation of dopamine D2 receptors. Proc Natl Acad Sci U S A. 1991; 88:3135–9. [PubMed: 1849644]
35. Shibata T, Suzuki C, Ohnishi J, Murakami K, Miyazaki H. Identification of regions in the human angiotensin II receptor type 1 responsible for Gi and Gq coupling by mutagenesis study. Biochem Biophys Res Commun. 1996; 218:383–9. [PubMed: 8573166]
36. Henry AG, White IJ, Marsh M, von Zastrow M, Hislop JN. The role of ubiquitination in lysosomal trafficking of delta-opioid receptors. Traffic. 2011; 12:170–84. [PubMed: 21106040]
37. Formstecher E, et al. Protein interaction mapping: a Drosophila case study. Genome Res. 2005; 15:376–84. [PubMed: 15710747]
38. Urbe S, et al. The UIM domain of Hrs couples receptor sorting to vesicle formation. J Cell Sci. 2003; 116:4169–79. [PubMed: 12953068]
39. Raiborg C, et al. FYVE and coiled-coil domains determine the specific localisation of Hrs to early endosomes. J Cell Sci. 2001; 114:2255–63. [PubMed: 11493665]
40. Bishop N, Horman A, Woodman P. Mammalian class E vps proteins recognize ubiquitin and act in the removal of endosomal protein-ubiquitin conjugates. J Cell Biol. 2002; 157:91–101. [PubMed: 11916981]
41. Russell M, Johnson GL. G protein amino-terminal alpha i2/alpha s chimeras reveal amino acids important in regulating alpha s activity. Mol Pharmacol. 1993; 44:255–63. [PubMed: 8394989]
42. Steinberg SF. Focus on “targeted expression of activated Q227L G(alpha)(s) in vivo”. Am J Physiol Cell Physiol. 2002; 283:C383–5. [PubMed: 12107046]
43. Berlot CH. A highly effective dominant negative alpha s construct containing mutations that affect distinct functions inhibits multiple Gs-coupled receptor signaling pathways. J Biol Chem. 2002; 277:21080–5. [PubMed: 11927592]
44. Daaka Y, et al. Essential role for G protein-coupled receptor endocytosis in the activation of mitogen-activated protein kinase. J Biol Chem. 1998; 273:685–8. [PubMed: 9422717]
45. McDonald PH, et al. Beta-arrestin 2: a receptor-regulated MAPK scaffold for the activation of JNK3. Science. 2000; 290:1574–7. [PubMed: 11090355]
46. Lefkowitz RJ, Shenoy SK. Transduction of receptor signals by beta-arrestins. Science. 2005; 308:512–7. [PubMed: 15845844]
47. Futahashi Y, et al. Separate elements are required for ligand-dependent and -independent internalization of metastatic potentiator CXCR4. Cancer Sci. 2007; 98:373–9. [PubMed: 17270027]
48. Zhang Y, et al. Intracellular localization and constitutive endocytosis of CXCR4 in human CD34+ hematopoietic progenitor cells. Stem Cells. 2004; 22:1015–29. [PubMed: 15536192]
49. Trapaidze N, Gomes I, Bansinath M, Devi LA. Recycling and resensitization of delta opioid receptors. DNA Cell Biol. 2000; 19:195–204. [PubMed: 10798443]
50. Sierra MI, Wright MH, Nash PD. AMSH interacts with ESCRT-0 to regulate the stability and trafficking of CXCR4. J Biol Chem. 2010; 285:13990–4004. [PubMed: 20159979]
51. Cho DI, et al. ARF6 and GASP-1 are post-endocytic sorting proteins selectively involved in the intracellular trafficking of dopamine D(2) receptors mediated by GRK and PKC in transfected cells. Br J Pharmacol. 2013; 168:1355–74. [PubMed: 23082996]
52. Thompson D, Whistler JL. Dopamine D(3) receptors are down-regulated following heterologous endocytosis by a specific interaction with G protein-coupled receptor-associated sorting protein-1. J Biol Chem. 2011; 286:1598–608. [PubMed: 21030592]

53. Heydorn A, et al. A library of 7TM receptor C-terminal tails. Interactions with the proposed post-endocytic sorting proteins ERM-binding phosphoprotein 50 (EBP50), N-ethylmaleimide-sensitive factor (NSF), sorting nexin 1 (SNX1), and G protein-coupled receptor-associated sorting protein (GASP). J Biol Chem. 2004; 279:54291–303. [PubMed: 15452121]
54. Wang Y, Zhou Y, Szabo K, Haft CR, Trejo J. Down-regulation of protease-activated receptor-1 is regulated by sorting nexin 1. Mol Biol Cell. 2002; 13:1965–76. [PubMed: 12058063]
55. Dores MR, et al. AP-3 regulates PAR1 ubiquitin-independent MVB/lysosomal sorting via an ALIX-mediated pathway. Mol Biol Cell. 2012; 23:3612–23. [PubMed: 22833563]
56. Kotowski SJ, Hopf FW, Seif T, Bonci A, von Zastrow M. Endocytosis promotes rapid dopaminergic signaling. Neuron. 2011; 71:278–90. [PubMed: 21791287]
57. Calebiro D, et al. Persistent cAMP-signals triggered by internalized G-protein-coupled receptors. PLoS Biol. 2009; 7:e1000172. [PubMed: 19688034]
58. Degtyarev MY, Spiegel AM, Jones TL. Increased palmitoylation of the Gs protein alpha subunit after activation by the beta-adrenergic receptor or cholera toxin. J Biol Chem. 1993; 268:23769–72. [PubMed: 8226908]
59. Mumby SM, Kleuss C, Gilman AG. Receptor regulation of G-protein palmitoylation. Proc Natl Acad Sci U S A. 1994; 91:2800–4. [PubMed: 8146194]
60. Wedegaertner PB, Bourne HR. Activation and depalmitoylation of Gs alpha. Cell. 1994; 77:1063–70. [PubMed: 7912657]
61. Wedegaertner PB, Bourne HR, von Zastrow M. Activation-induced subcellular redistribution of Gs alpha. Mol Biol Cell. 1996; 7:1225–33. [PubMed: 8856666]
62. Yu JZ, Rasenick MM. Real-time visualization of a fluorescent G(alpha)(s): dissociation of the activated G protein from plasma membrane. Mol Pharmacol. 2002; 61:352–9. [PubMed: 11809860]
63. Hynes TR, Mervine SM, Yost EA, Sabo JL, Berlot CH. Live cell imaging of Gs and the beta2-adrenergic receptor demonstrates that both alphas and beta1gamma7 internalize upon stimulation and exhibit similar trafficking patterns that differ from that of the beta2-adrenergic receptor. J Biol Chem. 2004; 279:44101–12. [PubMed: 15297467]
64. Allen JA, Yu JZ, Donati RJ, Rasenick MM. Beta-adrenergic receptor stimulation promotes G alpha s internalization through lipid rafts: a study in living cells. Mol Pharmacol. 2005; 67:1493–504. [PubMed: 15703379]
65. Weiss TS, et al. Galpha i3 binding to calnuc on Golgi membranes in living cells monitored by fluorescence resonance energy transfer of green fluorescent protein fusion proteins. Proc Natl Acad Sci U S A. 2001; 98:14961–6. [PubMed: 11752444]
66. Chaturvedi K, Bandari P, Chinen N, Howells RD. Proteasome involvement in agonist-induced down-regulation of mu and delta opioid receptors. J Biol Chem. 2001; 276:12345–55. [PubMed: 11152677]
67. Lachance V, et al. Regulation of beta2-adrenergic receptor maturation and anterograde trafficking by an interaction with Rab geranylgeranyltransferase: modulation of Rab geranylgeranylation by the receptor. J Biol Chem. 2011; 286:40802–13. [PubMed: 21990357]
68. Manders EM, Verbeek FJ, Aten JA. Measurements of objects in dual-color confocal images. J Microsc. 1993; 169:375–382.
69. Hislop JN, Henry AG, von Zastrow M. Ubiquitination in the first cytoplasmic loop of mu-opioid receptors reveals a hierarchical mechanism of lysosomal down-regulation. J Biol Chem. 2011; 286:40193–204. [PubMed: 21953467]
70. Garcia-Marcos M, Ghosh P, Farquhar MG. GIV is a nonreceptor GEF for G alpha i with a unique motif that regulates Akt signaling. Proc Natl Acad Sci U S A. 2009; 106:3178–83. [PubMed: 19211784]

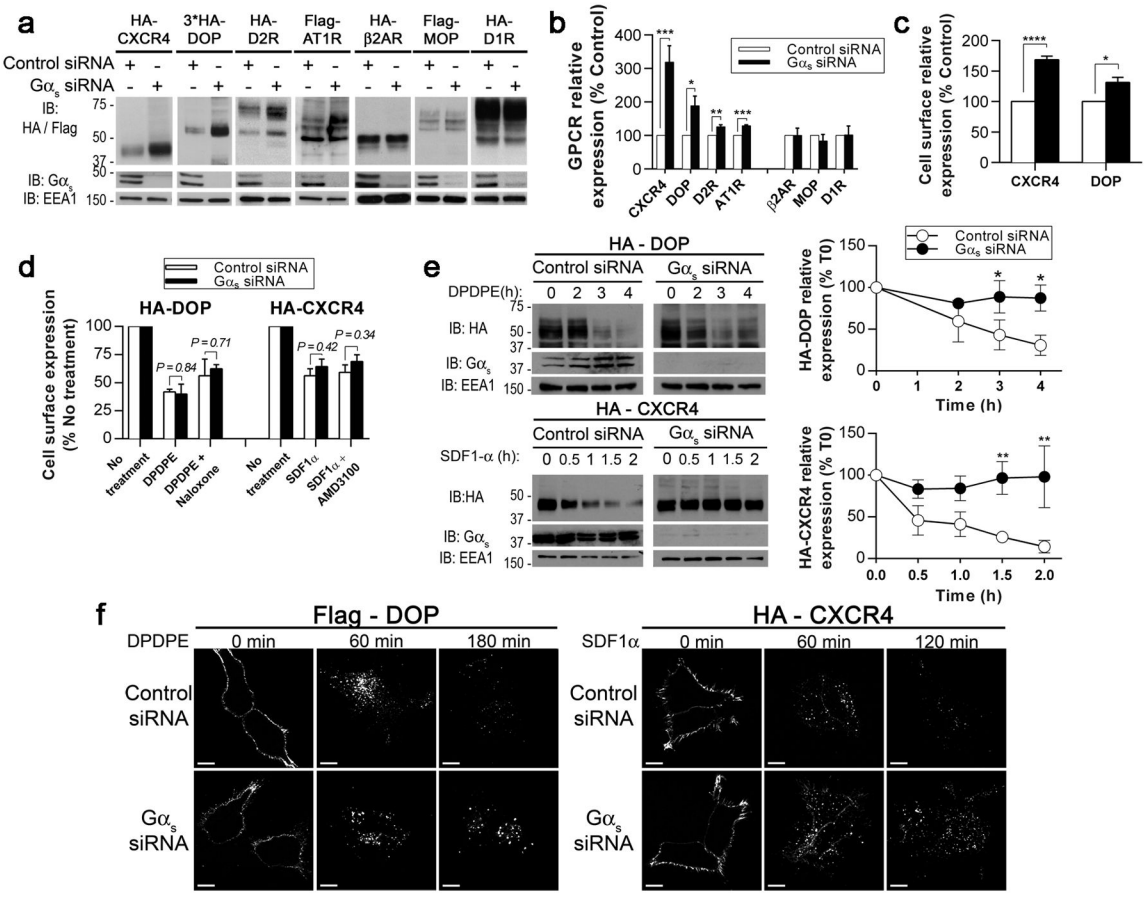

Fig. 1. $G\alpha_s$ knockdown delays GPCR degradation

(a) Representative immunoblots (IB) of the steady state levels of various tagged GPCRs transiently expressed in HEK293 cells treated with control or $G\alpha_s$ siRNA. EEA1, loading control. (b) Quantification of the GPCR expression in (a). The data are presented as the percentage of GPCR expression compared with control cells. GPCRs in the left part of the histogram have a higher propensity to down-regulate rather than to recycle and are not coupled to $G\alpha_s$ for signalling. (c) Quantification of the cell surface expression of HA-DOP and HA-CXCR4 in HEK293 cells treated with control or $G\alpha_s$ siRNA. ELISAs were performed to measure cell surface receptor expression. (d) Quantification of the internalisation and recycling rates of HA-DOP and HA-CXCR4 in cells treated with control or $G\alpha_s$ siRNA. ELISAs were performed to measure cell surface receptor levels in HEK293 cells that were untreated, treated with agonist (5 μM DPDPE or 100 nM SDF1-α) for 30 min (to measure internalisation) or treated with agonist followed by antagonist (10 μM naloxone or AMD3100) for 60 min (to measure recycling). Data are presented as the percentage of GPCR expression compared with untreated cells. (e) Representative immunoblots of the kinetics of Flag-DOP and HA-CXCR4 degradation following agonist stimulation in control or $G\alpha_s$-depleted HEK293 cells. Different film exposures were used for the control and $G\alpha_s$ siRNA blots to better show the differences in the degradation kinetics. (f) Quantification of the GPCR expression in (e). Data are presented as the percentage of GPCR expression compared with unstimulated cells (T0). (g) Immunofluorescence analysis of Flag-DOP and

HA-CXCR4 internalisation in HEK293 cells transfected with control or $G\alpha_s$ siRNA. Cell surface GPCRs were labelled with anti-Flag or anti-HA at 4°C before incubation at 37°C in the presence of agonists. At the indicated times, cells were processed for confocal microscopy analysis. For each time point, images were acquired using identical instrument settings. Scale bars, 10 μm. The data in (b), (c), (d) and (f) are presented as the mean±SEM of ≥3 independent experiments. Statistical analysis was performed by Student's *t* test. * $p \leq 0.05$, ** $p \leq 0.01$, *** $p \leq 0.001$, **** $p \leq 0.0001$.

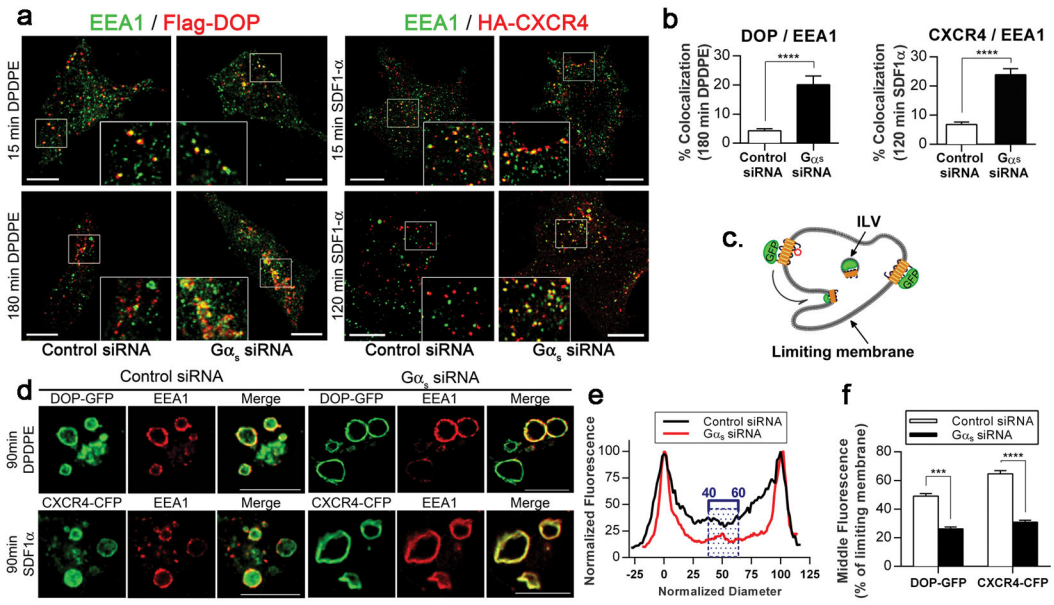

Fig. 2. Gα$_s$ knockdown alters the transfer of GPCRs to the ILVs of MVBs

(a) Gα$_s$ depletion prolonged the presence of internalised Flag-DOP and HA-CXCR4 in early endosomes. Confocal microscopy images comparing the distribution of the early endosome marker EEA1 and the cell surface labelled Flag-DOP and HA-CXCR4 in control or Gα$_s$-depleted HEK293 cells treated with agonist for 15, 120 or 180 min. Scale bars, 10 μm. The images were acquired at different laser and PMT settings to enable the detection of the GPCRs at each time point and to compare their localisation with EEA1. (b) Quantification of the degree of overlap between EEA1 and HA-CXCR4 or HA-DOP in cells treated with control or Gα$_s$ siRNA. (c) Diagram illustrating the distribution of a GPCR with a C-terminal GFP tag on the outer membrane of an endosome and in ILVs. (d) Gα$_s$ depletion prevented the redistribution of DOP-GFP and CXCR4-CFP from the endosome limiting membrane to the ILVs. Representative optical sections depict endosomes in control and Gα$_s$-depleted HEK293 cells co-transfected with DOP-GFP or CXCR4-CFP along with Rab5Q79L (to create enlarged endosomes) and treated with agonist for 90 min. Cells were fixed and processed for confocal microscopy. Scale bars, 10 μm. (e) Representative line scan analysis to quantify GPCR-GFP localisation to the ILVs of endosomes. The normalised diameter represents the diameter of the endosome, where 0 and 100 correspond to the pixel distances with the first and second maximum pixel intensities, signifying the limiting membranes of the endosomes. The black and red traces represent the normalised fluorescence pixel intensity measured across the endosomes in control and Gα$_s$-depleted cells, respectively, with the maximum pixel intensity across the line normalised to 100. The hatched box highlights the normalised fluorescence values of pixels from 40 to 60% of the normalised diameter that were used to determine the mean intraluminal fluorescence for each endosome. (f) Compiled results of the line scan analysis for DOP-GFP and CXCR4-CFP. The data in (b) and (f) are presented as the mean±SEM of n≥100 cells or endosomes, respectively, from three independent experiments. Statistical analysis was performed by Student's *t* test. ***p<0.001, **** p≤0.0001.

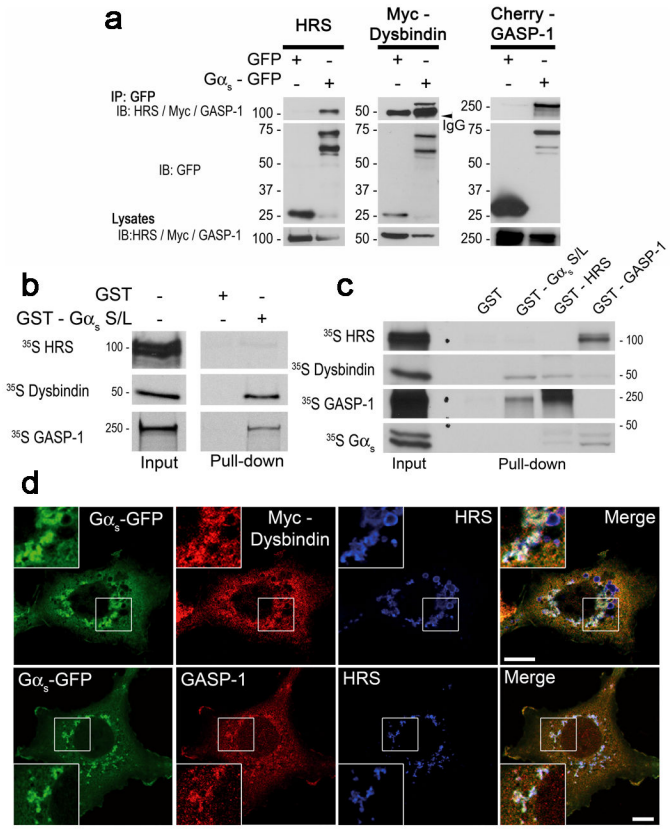

Fig. 3. Gα$_s$ interacts and colocalises with the GASP-1-dysbindin-HRS endosomal sorting machinery

(a) Immunoprecipitation of Gα$_s$-GFP with HRS, Myc-dysbindin and Cherry-GASP-1. Lysates from HEK293 cells transiently transfected with GFP or Gα$_s$-GFP along with HRS, Myc-dysbindin or Cherry-GASP-1 were immunoprecipitated (IP) with anti-GFP and immunoblotted (IB) using the indicated antibody. (b) GST pull-down experiment demonstrating that dysbindin and GASP-1, but not HRS, interact directly with Gα$_s$. *In vitro* translated ^{35}S-labelled dysbindin and GASP-1 bound to GST-Gα$_s$ (short (S) and long (L) forms) but not to GST. ^{35}S-labelled HRS did not bind to GST-Gα$_s$. Bound proteins were separated by SDS-PAGE and detected by autoradiography. (c) GST pull-down experiments to define the protein complex containing GASP-1, dysbindin, HRS and Gα$_s$. *In vitro* translated ^{35}S-labelled HRS, dysbindin, GASP-1 and Gα$_s$ were incubated with GST alone, GST-Gα$_s$, GST-HRS or GST-GASP-1. The samples were analysed as in (b). (d) Immunofluorescence analysis of COS7 cells transfected with Gα$_s$-GFP and Myc-dysbindin or Cherry-GASP-1. The cells were fixed, labelled with anti-GFP, anti-HRS and anti-Myc or anti-Cherry and then processed for confocal microscopy. The overexpression of Gα$_s$ together with dysbindin or GASP-1 promoted the formation of clustered and enlarged endosomes. Merged images illustrate the colocalisation of Gα$_s$, endogenous HRS and dysbindin or GASP-1 on endosomes. Scale bars, 10 μm.

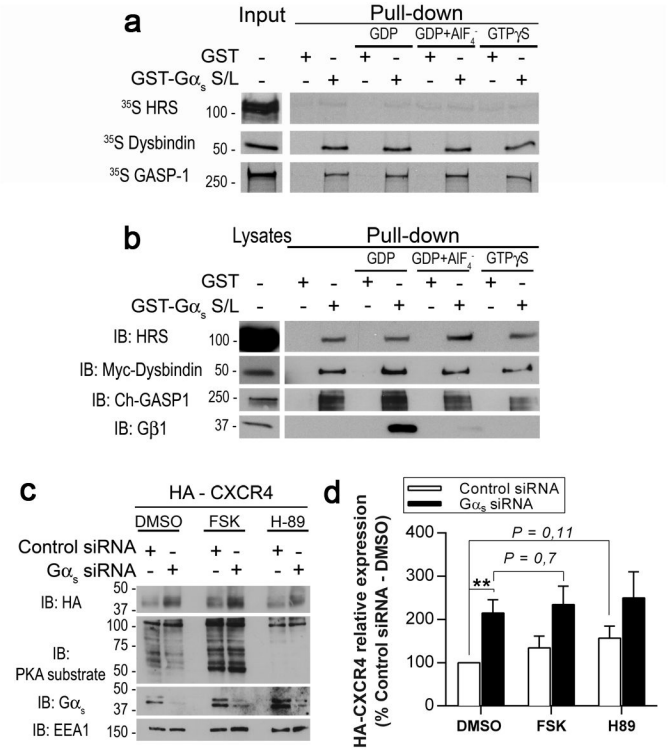

Fig. 4. The interaction of Gα$_s$ with the GPCR endosomal sorting machinery is independent of the activation status of Gα$_s$

(a) *In vitro* GST pull-down experiment showing that the Gα$_s$ activation state did not influence its direct interactions with HRS, dysbindin and GASP-1. *In vitro* translated ^{35}S-labelled HRS, dysbindin and GASP-1 were incubated with GST alone or GST-Gα$_s$ preloaded with GDP (to mimic the inactive state) or GDP/AlF4- or GTPγS (to mimic the active state). Bound proteins were separated by SDS-PAGE and detected by autoradiography. (b) GST pull-down experiment in cell lysates demonstrating that the interactions between overexpressed dysbindin, GASP-1 and HRS were independent of the GST-Gα$_s$ activation state. Lysates from HEK293 cells transiently transfected with HRS, Myc-dysbindin or Cherry-GASP-1 were incubated with GST alone, inactive GST-Gα$_s$-GDP or active GST-Gα$_s$-GDP/AlF4- or GTPγS (as described in (a)). Bound proteins were analysed by immunoblotting (IB) for HRS, Myc (dysbindin) and Cherry (GASP-1). The interaction with Gβ1 served as a control to confirm the activation state of GST-Gα$_s$ because Gβ1 only binds to inactive Gα$_s$. This control was included in each experiment in (a) and (b). (c) The downstream effectors of Gα$_s$ were not involved in CXCR4 down-regulation. Control and Gα$_s$-depleted HEK293 cells expressing HA-CXCR4 were treated for 8 h with vehicle (DMSO), 10 μM forskolin (an adenylyl cyclase activator) or 10 μM H89 (a PKA inhibitor). The steady state levels of HA-CXCR4 were analysed by immunoblotting using the indicated antibody. (d) Quantification of the HA-CXCR4 levels in (c). The data are presented as the percentage of HA-CXCR4 compared with control siRNA cells treated with DMSO. The data are presented as the mean±SEM of ≥3 independent experiments and statistical analysis was performed by Student's *t* test. ** p≤0.01.

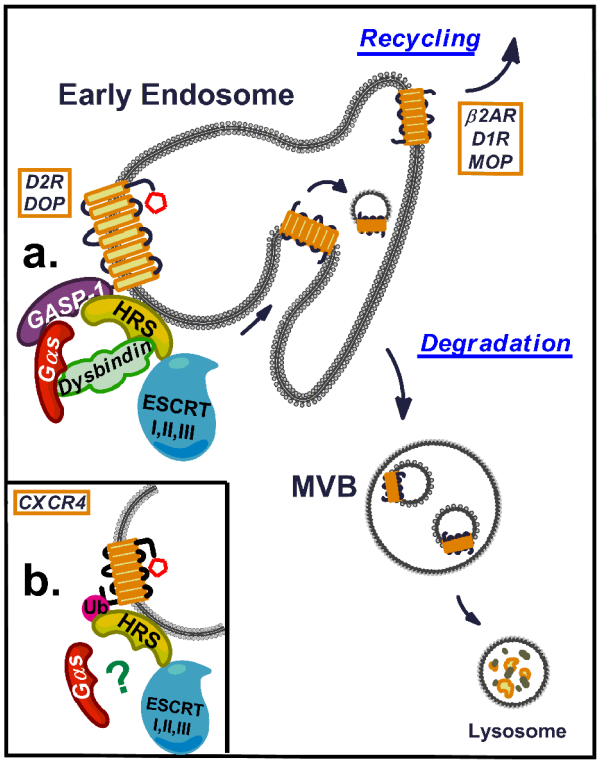

Fig. 5. Model for $G\alpha_s$ regulation of GPCR endosomal sorting

$G\alpha_s$ promotes the endosomal sorting of GPCRs into the ILVs of MVBs via the ESCRT machinery. (a) $G\alpha_s$ interacts directly with GASP-1 and dysbindin on endosomal membranes and facilitates/stabilises their downstream interactions with HRS and the ESCRT machinery. These interactions promote the endosomal sorting and down-regulation of a subset of GPCRs, such as DOP and D2R, for which ESCRT-sorting is ubiquitination-independent. (b) $G\alpha_s$ is also required for the endosomal sorting of GPCRs, such as CXCR4, that are sorted by the ubiquitin- and HRS-mediated ESCRT machinery but are independent of GASP-1 and dysbindin. However, the molecular components of the $G\alpha_s$-regulated CXCR4 endosomal sorting machinery have yet to be identified.